Study by XPS and UV−Visible and DRIFT Spectroscopies of Electropolymerized Films of Substituted Ni(II)-*p*-Phenylporphyrins and -Phthalocyanines

Cristhian Berríos,[†] José F. Marco,[‡] Claudio Gutiérrez,[‡] and María Soledad Ureta-Zañartu*,[†]

Facultad de Química y Biología, Universidad de Santiago de Chile (USACH), Casilla 40, Correo 33, Santiago, Chile, and Instituto de Química Física "Rocasolano", CSIC, C. Serrano, 119, 28006-Madrid, Spain

Received: May 26, 2008; Revised Manuscript Received: July 15, 2008

Films of nickel tetrasulfophthalocyanine and -*p*-phenylporphyrin (NiTSPc and NiTSPP, respectively) were obtained by repetitive cyclic voltammetry (RCV) of the 1 mM complex in aqueous solution, while films of the water-insoluble nickel tetraaminophthalocyanine and -*p*-phenylporphyrin (NiTAPc and NiTAPP, respectively) had to be obtained by RCV of the 1 mM complex in organic solvents. Glassy carbon (GC), ITO, or platinum electrodes were used as substrates. The modified electrodes were characterized by cyclic voltammetry (CV) and UV−visible, infrared, and X-ray photoelectron spectroscopies. The CVs of the sulfo films showed the characteristic peaks of the Ni(II)/Ni(III) process, whereas the CVs of the amino films did not, very small Ni(II)/Ni(III) peaks appearing only after activation by RCV. Upon oxidation to Ni(III) both sulfo films changed from transparent to dark violet. The IR spectra of the polyNiTSPP and the polyNiTSPc films showed bands at 3628 cm^{-1} and 3500 cm^{-1}, respectively, which could be due to interstitial water molecules occluded during the polymerization. The Ni 2p XP spectra indicate that the magnetic character of the Ni(II) ions in NiTSPP is dramatically changed by the polymerization, from diamagnetic in the monomer to paramagnetic in the polymeric film, indicating the formation of Ni−O−Ni bridges or of clusters of $Ni(OH)_2$. On the contrary, the Ni 2p XP spectra of the unactivated NiTAPP film, in which the Ni(II)/Ni(III) process was absent, showed only diamagnetic Ni(II). Therefore, it is concluded that only paramagnetic Ni(II) ions can be electrooxidized to Ni(III).

1. Introduction

The electrochemical applications of metallic phthalocyanines and porphyrins have been extensively studied,[1] especially as modified electrodes with activity for diverse oxidation reactions which could be the basis of electrochemical sensors.[2] Porphyrins[3] (P) and phthalocyanines[4] (Pc) can form thermodynamically stable supramolecular systems thanks to weak and exchange interactions. The completely flat aromatic skeleton of soluble sulfonated phthalocyanines and porphyrins allows them to form columnar aggregates in which π-stacking interactions between the monomers predominate.[5]

Nickel tetraazamacrocycles are exceptionally efficient and selective electrocatalysts, probably because nickel easily changes from a square planar to an octahedral conformation.[6] Repetitive cyclic voltammetry (RCV) in alkaline solution of a soluble macrocycle on an inert substrate yields at higher potentials, at which Ni(II) is oxidized to Ni(III) and the first steps of oxygen evolution occur, polymeric films that become firmly attached to the substrate.[7–10] Bukowska et al.[11] found in surface-enhanced Raman spectra of roughened gold electrodes modified with Ni-tetraazamacrocyclic complexes a doublet at 480/570 cm^{-1} which appeared at high potentials only and which they assigned to the symmetric and antisymmetric O−Ni(III)−O stretching vibrations of oxo bridges connecting the layers of the macrocycles. Perez-Morales et al.[12] found that the UV−visible absorbance spectrum of a polyNiTSPP film increased upon electrooxidation from the Ni(II) to the Ni(III) state. El-Nahass et al.[13] have reported the FTIR spectra in the region between 400 and 1000 cm^{-1} of the NiPc monomer and the transmission FTIR and UV−visible spectra of both as-deposited and annealed films at 573 K of NiPc evaporated in vacuum onto optically flat KBr and silica substrates, respectively.

The Ni(II)-porphyrin or -phthalocyanine monomers polymerize to form different structures, depending on their peripheral substituent. In a previous work[14] we characterized by UV−visible, FTIR, and XP spectroscopies, and quantum-chemical methods the monomers of Ni(II)-phthalocyanine (Pc) with *p*-amino- or -sulfonate substituent groups and of Ni(II)-phenylporphyrin (PP) with *p*-amino- or -sulfonate substituent groups. The sites more probable to undergo oxidation or reduction in the gas phase were suggested to be localized on the ligand rather than on the nickel atom, and consequently polymerization should occur through ligand sites.

Following the work with the monomers, the purpose of the present work is to achieve a better understanding of the electroformation of polymeric films of Ni(II)-porphyrins and -phthalocyanines, by means of XPS and UV−visible and FTIR spectroscopies and cyclic voltammetry.

2. Experimental Section

As in our previous work with the monomers,[14] two water-soluble (Ni-tetrasulfophthalocyanine (NiTSPc) and Ni-tetra-*p*-sulfophenylporphyrin (NiTSPP)) and two water-insoluble (Ni-tetraaminophthalocyanine (NiTAPc) and Ni-tetra-*p*-aminophenylporphyrin (NiTAPP)) Ni(II)-tetraaza complexes were used. NiTSPc (Aldrich), NiTSPP, NiTAPc, and NiTAPP (MID-Century, Posen, IL) and all other chemicals (Merck, p.a.) were used as received. The solutions of the sulfo monomers were prepared with deionized and twice-distilled

* Corresponding author.
[†] Universidad de Santiago de Chile (USACH).
[‡] Instituto de Química Física "Rocasolano".

10.1021/jp8046455 CCC: $40.75
Published on Web 09/13/2008

TABLE 1: Experimental Conditions Used for Electropolymerization of the Macrocycle Monomers on Glassy Carbon (concentration of the monomer: 1 mM)

monomer	electrolyte for polymerization	potential range, V_{MSE}	potential cycles for polymerization	stabilization (sulfo)/activation (amino) cycles at the pH shown	
				CVs	pH
NiTSPP	pH 11 buffer	−0.20 → 0.85	20	5	11
NiTSPc	0.1 M NaOH	−0.20 → 0.60	20	5	11
NiTAPc	1 mM TBAP in DMF	−0.20 → 0.55	20	80	13
NiTAPP	1 mM TBAP in ACN	−0.50 → 0.45	20	80	11

water and stored in a dark bottle, their stability being checked before use by the invariance of the UV−vis spectra. The modified electrodes were prepared as described,[9] namely, a glassy carbon (GC) (Pine Instruments, 0.8 cm in diameter), indium tin oxide (ITO) (Delta Technologies Ltd.), or Pt foil (Aldrich) electrode was subjected to repetitive cyclic voltammetry (RCV) at 10 mV s^{-1} between the potential limits (vs mercurous sulfate electrode (MSE), 0.64 V vs SHE) and using the electrolyte solutions shown in Table 1, at room temperature and under nitrogen atmosphere. ITO electrodes were used for UV−vis spectroscopy and XPS, and a platinum sheet for specular reflectance FTIRS. It is known[9,10] that the nature of the substrate (GC, Pt, Au, or ITO) does not significantly affect the electrochemical behavior of the films.

The polyNi-macrocycle/GC (or /Pt or /ITO) electrodes were characterized by cyclic voltammetry (CV) at 0.1 V s^{-1} in a pH 11 carbonate/hydrogen carbonate buffer electrolyte. As the peak current of the Ni(II)/Ni(III) process was not proportional to the scan rate (i.e., the process involved only a fraction of the Ni atoms in the film), the surface loading is expressed as the peak current density (PCD) at 0.1 V s^{-1} of Ni(II) electrooxidation, as described for polyNiTSPc/Au electrodes,[10] for which a PCD of 0.5 mA cm^{-2} corresponded to a thickness of about 25 nm as estimated by EQCM.[15]

The electrochemical equipment has been described.[9] For UV−vis spectroscopy, a double-beam Varian UV−vis spectrophotometer, model Cary 1E, was used. Spectra of the monomers in the pH 11 buffer were obtained with 1 cm silica cells, using the pH 11 buffer as a blank, and spectra of the films were obtained with spectroelectrochemical silica cells of 1.5 cm optical length with an ITO working electrode, a Pt wire auxiliary electrode, and a Ag/AgCl reference electrode (although the potential is referred to the MSE in order to facilitate comparison with the CVs with GC substrate) and using as blank an identical cell with an ITO electrode in the pH 11 buffer. IR spectra were obtained with a Bruker IFS 66v FTIR-spectrometer at a pressure of 14 mbar. Transmittance spectra of the monomers in KBr pellets (reference: pure KBr pellets), and ex situ specular reflectance spectra (reference: bare Pt sheet) at an incidence angle of 45° of polymer films deposited on Pt were obtained. XPS data were recorded with a triple channeltron CLAM2 analyzer at a vacuum in the range 10^{-9} mbar, using Mg Kα radiation and a constant analyzer transmission energy of 20 eV. All the spectra were recorded at takeoff angles of 90°, and all binding energies were referenced to the main C 1s signal of porphyrin at 284.8 eV.

3. Results and Discussion

3.1. Preparation and Voltammetric Characterization of PolyNi-macrocycle-GC Electrodes by Repetitive Cyclic Voltammetry (RCV). The first 20 CVs at 0.01 V s^{-1} of electropolymerization of the four monomers are shown in Figure 1 (thin lines). In all cases there is a non-Nernstian process whose currents increase with cycling because of film growth. During the polymerization of the sulfo complexes, oxygen evolution shifts to less positive potentials, showing the electrocatalytic activity of the films for this process (Figure 1A and 1B). Previous EQCM results show that a considerable amount of water leaves the film upon the oxidation of Ni(II) to Ni(III).[10] This dehydration probably collaborating in the formation of a stacked structure via Ni−O−Ni oxo bridges.[7] While polyNiTSPP could be grown in the pH 11 buffer, polyNiTSPc had to be prepared in a strongly alkaline solution, 0.1 M NaOH. Even so, for the same number of electropolymerization cycles, the currents of the Ni(II)/Ni(III) process were about twice as high for NiTSPP, demonstrating an easier film formation. Stabilized CVs of both polyNiTSPP and polyNiTSPc (thick lines in Figures 1A and 1B, respectively) in the pH 11 buffer electrolyte were obtained after five RCVs at 0.1 V s^{-1} in this electrolyte and have been already described.[15]

CVs at 0.01 V s^{-1} of 1 mM NiTAPP on a GC electrode in ACN with 1 mM TBAP show a very non-Nernstian process, whose anodic and cathodic peaks initially appear at about 0.4 and −0.1 V, respectively (Figure 1C). Both peaks increase with cycling owing to film formation, probably produced by irreversible oxidation of the amino groups at potentials above 0.50 V. CVs at 0.01 V s^{-1} of 1 mM NiTAPc in DMF with 1 mM TBAP show in the first positive scan a shoulder at about 0.0 V and a peak at 0.39 V vs MSE (Figure 1D), but only one cathodic peak, all the peaks increasing with cycling.

After formation of the film, the amino-modified electrodes were carefully rinsed with water, transferred to the pH 11 buffer (polyNiTAPP) or to 0.1 M NaOH (polyNiTAPc) and activated by 80 RCVs. The CVs in the pH 11 buffer after this activation are shown in Figures 1C and 1D, respectively (thick lines). The

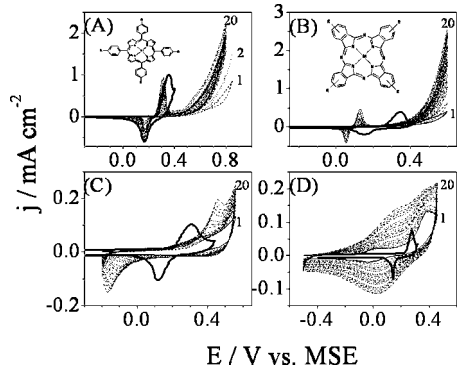

Figure 1. First 20 RCVs (thin lines) at 0.01 V s^{-1} in 1 mM Ni(II) monomer of (A) NiTSPP in the pH 11 buffer, (B) NiTSPc in 0.1 M NaOH, (C) NiTAPP in ACN, and (D) NiTAPc in DMF. The thick lines are the CVs of the polymeric films in the pH 11 buffer: polyNiTSPP (A) and polyNiTSPc (B), both after five stabilization RCVs in the pH 11 buffer; (C) polyNiTAPP after activation by 80 RCVs in the pH 11 buffer, and (D) polyNiTAPc after activation by 80 RCVs in 0.1 M NaOH. Insets: Structure of the monomers: (A) Ni(II)phenylporphyrin and (B) Ni(II)phthalocyanine; in both monomers, R can be SO_3^- or NH_2.

TABLE 2: Cyclic Voltammetric Parameters of the Two Stabilized Sulfo Films and of the Two Activated Amino Films

	polyNiTSPP at 1.0 PCD mA cm^{-2}		polyNiTSPc at 0.71 PCD mA cm^{-2}		polyNiTAPP at 0.07 PCD mA cm^{-2}		polyNiTAPc at 0.20 PCD mA cm^{-2}	
parameter	anodic	cathodic	anodic	cathodic	anodic	cathodic	anodic	cathodic
$dj_p/dv^{0.5}$ mA s$^{1/2}$ V$^{-1/2}$ cm^{-2}	3.80 ± 0.13	2.14 ± 0.07	2.44 ± 0.03	1.22 ± 0.04	0.20 ± 0.04	0.20 ± 0.006	0.83 ± 0.03	0.61 ± 0.02
$(Ep)_{v=1\ mV/s}$	0.37	0.17	0.40	0.14	0.34	0.13	0.36	0.16
$dE_p/d \log v$ (V/dec)	0.027 ± 0.004	−0.021 ± 0.02	0.049 ± 0.02	−0.030 ± 0.004	0.035 ± 0.002	−0.037 ± 0.003	0.037 ± 0.002	−0.024 ± 0.003

TABLE 3: Wavelength Maxima (nm) of the Bands in the Transmission UV-vis Spectra of the Different Monomers in Solution and of the Corresponding Polymerized Films on ITO from Figures 2 and 3

	complex in solution		reduced film		oxidized film	
	Soret band	Q-band	Soret band	Q-band	Soret band	Q-band
NiTSPc	336	625 dimer, 665 monomer	333	597	334	592
NiTSPP	405	527	408	522	407	521
NiTAPc	310	726	313	726	–	–
NiTAPP	422	534	422	534	–	–

currents of the activated amino-modified electrodes are very low, indicating that only a small fraction of the Ni atoms can be activated, but the double-layer currents are high, demonstrating a higher thickness (or a higher porosity) as compared with the sulfo films.[15]

It has been proposed that both the Ni-aminophenylporphyrin and the Ni-aminophthalocyanine monomers polymerize through the irreversible oxidation of the amino groups. So, White and Murray[16] studied the oxidation of nonmetalated tetraamino-*o*-phenylporphyrin (H_2(*o*-TAPP)) and of several of its metalated derivatives on Pt in acetonitrile and postulated an aniline-like polymerization initiated by oxidation of the NH_2 groups. Li and Guarr[17] also postulate that the first oxidation in NiTAPc is that of the ligand.

Table 2 shows some parameters obtained from CVs at scan rates (v) from 5 to 300 mV s^{-1}. As already reported,[9] for polyNiTSPc-modified GC electrodes $d \log(j_p)/d \log(v)$ decreases with increasing film thickness, from 0.85 to 0.50, indicating that, as could be expected, diffusion control was obtained for thicker films and higher scan rates. (This trend had been already noted by White and Murray.[16]) For $v > 0.02$ the slope $d \log(j_p)/d \log(v)$ is 0.5 for all the studied systems, and the j_p vs $\sqrt{v}$ plots are linear and pass through the origin, i.e., the process is diffusion-controlled at these higher scan rates, at which charge transfer in the film does not have time to reach the film/electrolyte interface, so that, in effect, the film acts as a semi-infinite medium. The $dj_p/dv^{0.5}$ slopes for the amino complexes are considerably lower than those for the sulfo complexes (Table 2), probably because of the lower concentration of Ni active centers in the former. The $d(E_p)/d \log(v)$ slopes range from 27 to 49 mV dec^{-1} for the anodic peak and from 21 to 37 mV dec^{-1} for the cathodic peak. When the process is diffusion-controlled (within the polymer bulk, without reaching the film/electrolyte interface), the corresponding Tafel slopes are mostly in the range of 60 mV dec^{-1}, suggesting that one electron is transferred before a chemical rate-determining step.

3.2. UV−vis Spectroscopy. The transmission UV−vis spectra of the film/ITO electrodes at open circuit (thin solid lines) are very similar to, although broader than, those of the monomers (dashed lines in Figure 2). The wavelength maxima of both the Q and Soret bands barely shift from the monomer to the corresponding polymer, with the exception of the Q-band of NiTSPc, which in the polyNiTSPc films appears at 597 nm (Table 3), while in aqueous solution NiTSPc is mainly present as a dimer at 625 nm, the monomer appearing only as a shoulder at 665 nm.[18] The 0.016 mM concentration of the monomer corresponds to a surface concentration in the 1-cm cells of 16 nmol cm^{-2}. The absorbances of the sulfo films are about 1 order of magnitude lower than those of the corresponding monomers, while the absorbance of the amino films are comparable to those of the corresponding monomers, indicating that the amino films are thicker than the sulfo films, in spite of the higher currents of the latter. Assuming that both types of film have a similar porosity, this would be in agreement with the higher capacitive currents in the double layer region of the amino films (thick solid lines in Figure 1 C and D).

The absorbance of both sulfo films increases upon their oxidation to Ni(III) (thick solid lines in Figures 2A and 2B), so much so that a change from transparent to dark violet is visible to the naked eye. Upon opening the circuit, the absorbance decreases slowly down to its initial value for Ni(II), as already reported for polyNiTSPc,[9] the film recovering its initial transparency. As reported by Pérez-Morales et al. for polyNiTSPP,[12] this process can be repeated indefinitely, in agreement with the stability of the CV. No absorbance increase was obtained for the amino films, either fresh or activated, probably because in them only a small fraction of the Ni atoms is active.

The spectra of MPc complexes are due to electronic transitions from the highest occupied molecular orbital (HOMO) (π) to the lowest unoccupied molecular orbital (LUMO) (π^*), the Soret band being due to an $a_{2u}(\pi) \rightarrow e_g(\pi^*)$ transition and the Q-band to an $a_{1u}(\pi) \rightarrow e_g(\pi^*)$ transition.[19,20] In previous work with monomers,[14] we attributed the Soret band to both a HOMO-1(π)→LUMO(π^*) and a HOMO-1(π)→LUMO+1(π^*) transition, and the Q-band to both a HOMO(π)→LUMO(π^*) and a HOMO(π)→LUMO+1(π^*) transition, since the LUMO and LUMO + 1 orbitals have the same energy.

The deconvoluted UV−vis spectra of both reduced and oxidized polyNiTSPc (from Figure 2) are shown in Figure 3A and 3B, respectively. Only the small band at 478 nm in the reduced polymer, generally associated to a metal−ligand charge transfer, experiences a large shift, to 496 nm, upon oxidation, as well as a large intensity increase (Figures 3A and 3B).

3.3. Infrared Spectra. In Figure 4 we show the transmission spectra of the NiTSPP and NiTSPc monomers in KBr pellets (curves a and c, respectively), and the ex situ specular reflectance spectra of the polyNiTSPP and polyNiTSPc films on Pt (curves b and d, respectively). As expected, polymerization does not critically affect the spectra. Most of the bands associated with the skeleton of the ligands are present and have been identified in a previous work with the help of quantum-chemical calculations.[14] The band at 463 cm^{-1} shown by both sulfo films could

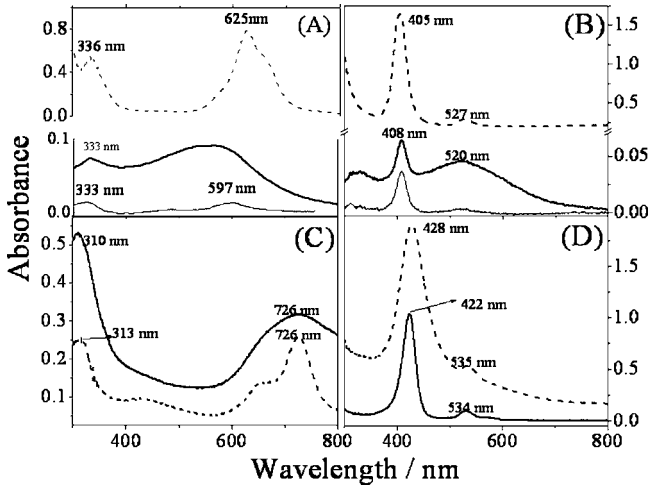

Figure 2. Dashed lines: UV−vis spectra of 0.016 mM solutions of the monomers in 1-cm cells: (A) NiTSPc in the pH 11buffer; (B) NiTSPP in the pH 11 buffer; (C) NiTAPc in ACN-TBAP; (D) NiTAPP in DMF-TBAP (dashed lines). Thin solid lines: UV−vis spectra of the corresponding polymeric films on ITO. The thick solid lines in A and B are the UV−vis spectra of the oxidized polyNiTSPc and polyNiTSPP films, respectively.

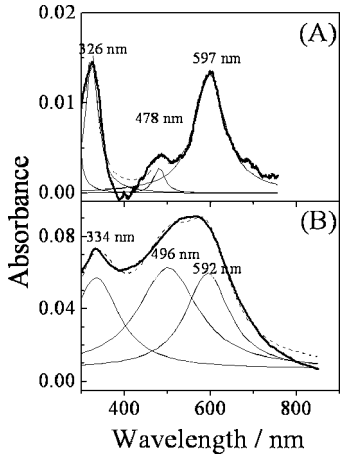

Figure 3. Deconvolution of the UV−vis spectra of films of (A) polyNi(II)TSPc; (B) polyNi(III)TSPc. Thick solid lines: experimental spectra; dashed lines: fitted curves; thin solid lines: deconvolution curves.

be the same found at 472 cm^{-1} by Pérez-Morales et al.[12] The sulfo monomers show a broad band centered at 3444 cm^{-1}, not reported in the literature because most spectra stop at 2000−3000 cm^{-1}, and probably due to water hydration of the Na^+ cations because the water of crystallization of both aliphatic and aromatic sodium sulfonates originates a band in this region.[21] The polyNiTSPP film has a band at 3628 cm^{-1}, and the polyNiTSPc film a band at 3500 cm^{-1}, in fair agreement with Pérez-Morales et al.,[12] who found bands at 3640 and 3540 cm^{-1}, respectively, in the specular reflectance spectrum of polyNiTSPP. These bands could also be due to interstitial water molecules occluded during the polymerization. In both sulfo films, new bands appear around 2900 cm^{-1}, which remain unassigned.

The transmission spectra of the amino monomers in KBr pellets and the ex situ specular reflectance spectra of the corresponding fresh and activated films on Pt are very similar (Figure 5). The amino monomers show weak bands at 3365 and 3220 cm^{-1} for NiTAPP and 3332 and 3214 cm^{-1} for NiTAPc, which for each compound corresponds, respectively, to the antisymmetric and symmetric stretching vibrations of the

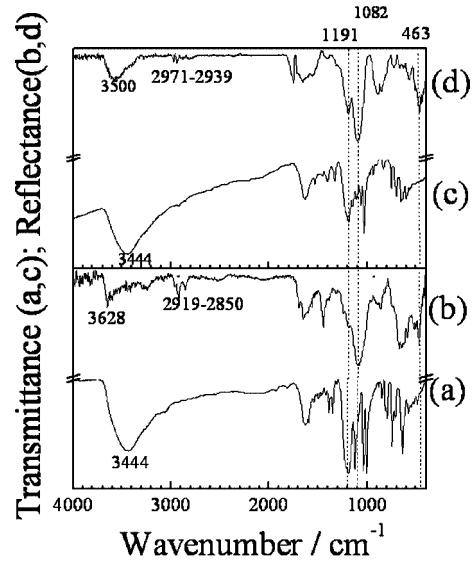

Figure 4. Transmittance FTIR spectra of NiTSPP (a) and NiTSPc (c) monomers as powder in KBr pellets, and ex situ specular reflectance FTIR spectra of Pt electrodes modified with films of polyNiTSPP/Pt (b) and polyNiTSPc/Pt (d).

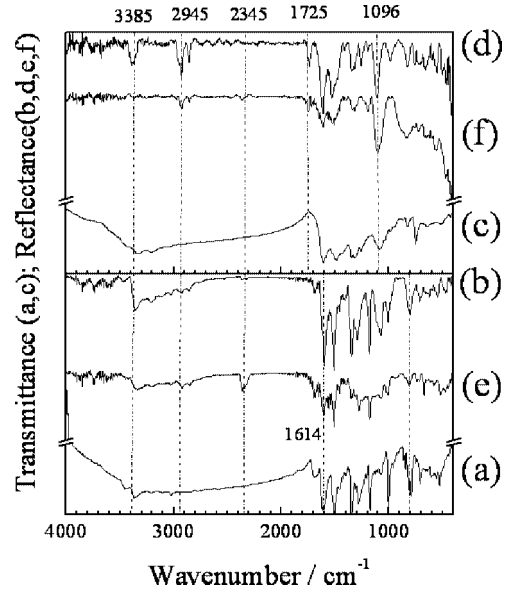

Figure 5. Transmittance FTIR spectra of NiTAPP (a) and NiTAPc (c) monomers as powder in KBr pellets, and ex situ specular reflectance FTIR spectra of Pt electrodes modified with: as-deposited (b and d) and activated (e and f) films of polyNiTAPP/Pt and polyNiTAPc/Pt, respectively.

NH_2 groups. The as-deposited amino films (spectra b and d) show a large band at 3385 cm^{-1}, which could be attributed to NH_2 groups forming intermolecular hydrogen bridges. However, this band tends to disappear upon activation of the amino films (spectra e and f), which runs contrary to the increase of the XPS peak attributed to NH_2 and/or NH (see below). The new band at 2945 cm^{-1} could not be assigned.

3.4. X-ray Photoelectron Spectroscopy (XPS). The Ni 2p XP spectra of the powdered NiTSPP monomer (Figure 6A), the polyNiTSPP film (Figure 6B), the polyNiTSPP film after 20 CVs (Figure 6C), the powdered NiTAPP monomer (Figure 6D), the polyNiTAPP film (Figure 6E), and the activated polyNiTAPP film (Figure 6F) are shown in Figure 6, and the binding energies (BEs) of all the peaks are collected in Table 4. The Ni 2p spectrum of the NiTSPP monomer consists, as

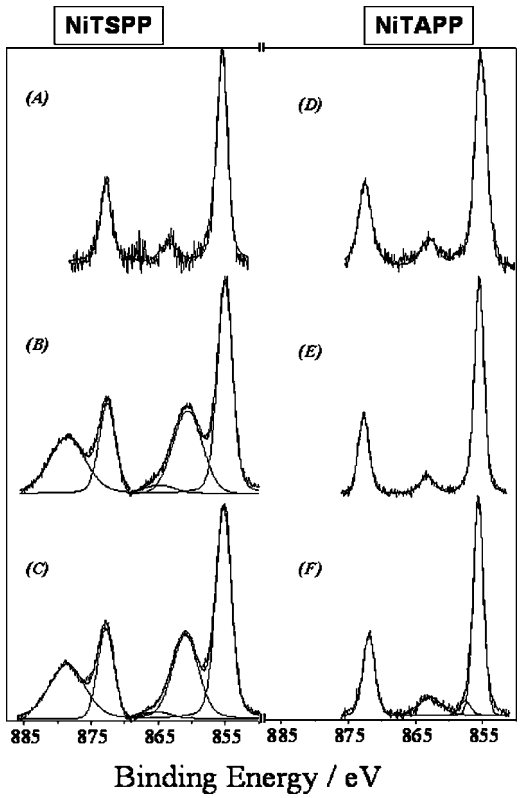

Figure 6. Ni2p XP spectra of (A) NiTSPP powder, (B) polyNiTSPP/ITO as-prepared, (C) polyNiTSSP/ITO after 20 CVs, (D) NiTAPP powder, (E) as-prepared polyNiTAPP/ITO, and (F) activated polyNiTAPP/ITO.

TABLE 4: Binding Energies (eV) of the Different Components of the Ni 2p XP Spectra of the Monomers and Films of NiTSPP and NiTAPP

sample	Ni $2p_{3/2}$	satellite 1	satellite 2	Ni $2p_{1/2}$	satellite 3
NiTSPP monomer	855.4	863.1		873.0	
polyNiTSPP	855.1	860.5	864.8	872.6	878.5
polyNiTSPP after 20 CVs	855.2	860.8	865.1	872.8	878.6
NiTAPP monomer	855.4	863.1		873.0	
polyNiTAPP	855.5	863.3		872.7	
polyNiTAPP, activated	855.6	862.8		871.8	

already reported,[14] of a relatively narrow spin−orbit doublet with BEs of the Ni $2p_{3/2}$ and Ni $2p_{1/2}$ core levels of 855.4 and 873.0 eV, respectively (Table 4), these values being similar to those for other Ni porphyrins.[22–24] The weak satellite at 863.1 eV is also in agreement with the literature.[25] The absence of strong shakeup satellite structure confirms the diamagnetic nature of Ni(II) in the TSPP monomer. Polymerization dramatically affects the spectrum, which now has a complex shape with intense shakeup satellite structure adjacent to the main photoemission peaks, indicating that the Ni(II) present in the polyNiTSPP film has become paramagnetic. This spectrum is very similar, although with 1 eV lower BEs, to those of a polyNiTSPc film and of $Ni(OH)_2$, which were practically undistinguishable.[9] Therefore, the spectrum is compatible with the presence of Ni−O−Ni bridges, although it is not possible to distinguish by XPS if they are present in clusters of an $Ni(OH)_2$-like phase within the polymeric film or to bridges between Ni atoms in parallel-stacked, contiguous layers of the macrocycle. The spectrum remains practically unchanged after 20 CVs (Figure 6C). In conclusion, the Ni(II) ions that participate in the Ni(II)/Ni(III) are paramagnetic.

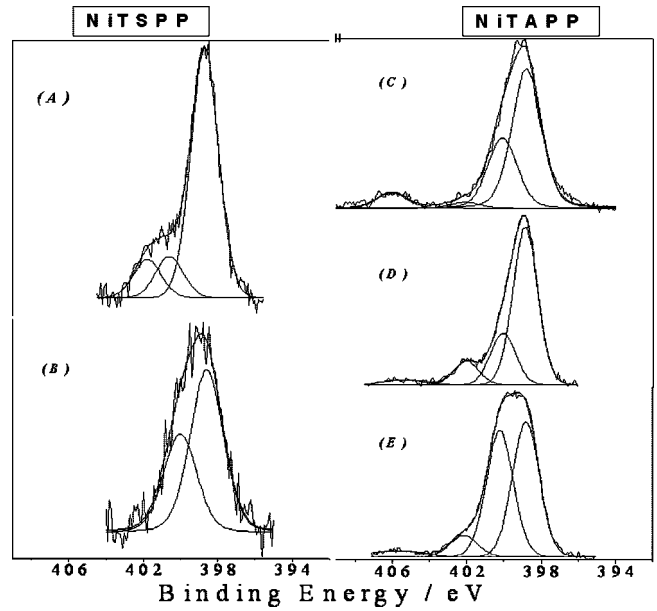

Figure 7. N1s XP spectra of: (A) NiTSPP powder, (B) polyNiTSPP/ITO, (C) NiTAPP powder, (D) as-prepared polyNiTAPc/ITO, (E) activated polyNiTAPP/ITO.

TABLE 5: Binding Energies and Relative Spectral Areas of the Different Components of the N 1s XP Spectra of the Monomers and Films of NiTSPP and NiTAPP

sample	BE (area)	BE (area)	BE (area)	BE (area)
NiTSPP monomer	398.8 (77%)	399.9 (11%)	401.5 (12%)	
polyNiTSPP	398.6 (62%)	400.0 (38%)		
NiTAPP monomer	398.8 (60%)	400.1 (30%)	402.1 (3%)	405.7 (7%)
polyNiTAPP	398.9 (65%)	400.0 (23%)	402.1 (9%)	405.7 (3%)
polyNiTAPP, activated	398.8 (46%)	400.2 (44%)	402.1 (7%)	405.7 (3%)

Contrary to NiTSPP, polymerization barely affects, if at all, the Ni 2p spectrum of NiTAPP, which is practically the same for the film (Figure 6E) and the monomer (Figure 6D). The BEs of the main Ni $2p_{3/2}$ and Ni $2p_{1/2}$ core levels are 855.4 and 873.0 eV, respectively, and there is a very weak satellite at 863.1 eV (Table 4). The near absence of a strong shakeup structure indicates that the Ni(II) is mainly diamagnetic. The Ni 2p spectrum of the activated polyNiTAPP film (Figure 6F) shows a slight asymmetry in the high BE side of the main Ni $2p_{3/2}$ line and, also, a change in the shape of the corresponding shakeup satellite, which broadens and shifts its position toward slightly lower BEs, this being compatible with a small paramagnetic Ni (II) contribution. The absence of the Ni(II)/Ni(III) process in the CV of unactivated polyNiTAPP, with diamagnetic Ni(II) ions only, and the very small current density of the Ni(II)/Ni(III) process in the CV of activated polyNiTAPP (Table 2), in parallel with the very small contribution of paramagnetic Ni(II) ions in the Ni2p XP spectrum, allow us to unequivocally conclude that only paramagnetic Ni(II) ions participate in the Ni(II)/Ni(III) process.

The N 1s spectrum of the NiTSPP monomer is shown in Figure 7A, and the BEs and relative spectral areas of the different components are collected in Table 5. The main peak (77% of the total spectral area) appears at 398.8 eV and is characteristic of the pyrrolic nitrogen in NiTSPP.[22] The minor peak at 399.9 eV (11%) is characteristic of the NH group in free-base (unmetalated) porphyrins and might arise from a small degree of demetalation induced by the X-rays[26] or to an unmetalated porphyrin impurity in the original sample. Finally, the minor peak at 401.5 eV (12%) could be due to high BE

nitrogen species, usually observed at 401.5−403.0 eV in the N 1s XP spectra of porphyrins[27–29] and associated with shakeup satellites.[30]

The N 1s spectrum of the polyNiTSPP film (Figure 7B) shows only two components: a major one of the pyrrolic nitrogen and a minor one of the NH groups (Figure 7B). The intensity of the NH component is 38%, much higher than that of 11% in the spectrum of the monomer, demonstrating that polymerization increases the proportion of NH groups. This favors the assumption that the Ni atoms in the polymer are no longer bonded to the macrocycle but have formed an independent, $Ni(OH)_2$-like phase, probably as clusters embedded in the polymer.

The N 1s spectrum of the NiTAPP monomer (Figure 7C) contains several contributions. The main one at 398.8 eV (60%) corresponds to the pyrrolic nitrogen bonded to Ni(II) in the porphyrin structure, while the contribution at 400.0−400.2 eV (30%) is associated with the NH_2 groups. Other minor components at higher BEs are due to shakeup satellites (402.1 eV, 3%) and inelastic scattering[30] (405.7 eV, 7%) (see also Table 5). The N 1s spectrum of the unactivated NiTAPP film (Figure 7D) is similar to that of the monomer, but for a small increase of the shakeup satellite and a slight decrease of the NH_2 component (see Table 5), this decrease suggesting that polymerization involves the NH_2 groups. On the contrary, the N 1s spectrum of the activated polyNiTAPP film (Figure 7E, Table 5) shows a remarkable increase of the peak of NH_2. Since the activation cannot increase the concentration of amino groups, the increase of the NH_2 peak suggests, taking into account the difficulty of distinguishing by XPS an NH_2 group from the NH group in the free-base porphyrin, that activation produces some demetalation with formation of $Ni(OH)_2$-like clusters. In effect, we have found no difference in BE between the peaks of the NH groups in unmetalated phthalocyanine, H_2Pc, and the peaks of the NH_2 groups of unmetalated tetraaminophenylporphyrin, H_2TAPP, in narrow-scan N 1s spectra.

4. Conclusions

The results obtained in this work allow us to conclude the following:

(1) The higher UV−vis absorbance and higher capacitive current densities of the polymeric amino films indicate that they are thicker than the sulfo films, despite the lower current densities of the Ni(II)/Ni(III) process of the former.

(2) The absorbance in the visible region of both sulfo films increased strongly upon their oxidation to Ni(III).

(3) The bands at 3628 cm^{-1} and 3500 cm^{-1} in the IR spectra of the polyNiTSPP and the polyNiTSPc films, respectively, could be due to interstitial water molecules occluded during the polymerization.

(4) The Ni 2p spectra clearly indicate a dramatic change in the magnetic nature of the Ni(II) ions in NiTSPP, from diamagnetic in the monomer to paramagnetic in the polymeric film, indicating the formation of an $Ni(OH)_2$-like phase or of Ni−O−Ni bridges.

(5) The N 1s spectra of NiTSPP show that the NH contribution is 3.5 times larger in the film than in the monomer, this demetalation suggesting again that the Ni(II) ions in the polymer have formed an independent, $Ni(OH)_2$-like phase.

(6) The Ni 2p spectrum of the unactivated NiTAPP film, which shows no Ni(II)/Ni(III) process, is practically identical to that of the diamagnetic monomer. The activated film, with only very small peaks of the Ni(II)/Ni(III) process, shows also only a very small paramagnetic contribution. Both facts give further, conclusive proof that only paramagnetic Ni(II) ions participate in the Ni(II)/Ni(III) process.

(7) The N 1s spectra of NiTAPP show that the NH_2 peak of the film becomes twice higher upon activation. Since it is difficult to distinguish by XPS the NH_2 from the NH contribution, this could also be due to a demetalation of the macrocycle due to the formation of $Ni(OH)_2$-like clusters.

Acknowledgment. The authors appreciate the financial support of DICYT-USACh and FONDECYT 1070290, as well as the CSIC (Spain)-USACh (Chile) joint program.

References and Notes

(1) Zagal, J. H. In *Handbook of Fuel Cells: Fundamentals, Technology and Applications*; Vielstich, W., Lamm, A., Gasteiger, H. A. , Eds.; Wiley: Chichester, 2003; Vol. 2.
(2) Oni, J.; Westebroek, P.; Nyokong, T. *Electroanalysis* **2003**, *15*, 847.
(3) Satake, A.; Kobuke, Y. *Tetrahedron* **2005**, *61*, 13.
(4) Agboola, B.; Ozoemena, K. I.; Nyokong, T. *J. Mol. Catal. A: Chem.* **2005**, *227*, 209.
(5) De Wael, K.; Westbroek, P.; Bultinck, P.; Depla, D.; Vandenabeele, P.; Adriaens, A.; Temmerman, E. *Electrochem. Commun.* **2005**, *7*, 87.
(6) Lever, A. B. P.; Hempstead, M. R.; Leznoff, C. C.; Liu, W.; Melnik, M.; Nevin, W. A.; Seymour, P. *Pure Appl. Chem.* **1986**, *58*, 1467.
(7) Trévin, S.; Bedioui, F.; Devynck, J. *J. Electroanal. Chem.* **1996**, *408*, 261.
(8) Trévin, S.; Bedioui, F.; Gomez.Villegas, M. G.; Bied-Charreton, C. *J. Mater.Chem.* **1997**, *7*, 923.
(9) Ureta-Zañartu, M. S.; Berríos, C.; Pavez, J.; Zagal, J.; Gutiérrez, C.; Marco, J. F. *J. Electroanal. Chem.* **2003**, *553*, 147.
(10) Ureta-Zañartu, M. S.; Alarcón, A.; Berríos, C.; Cárdenas-Jirón, G. I.; Zagal, J.; Gutiérrez, C. *J. Electroanal. Chem.* **2005**, *580*, 94.
(11) Bukowska, J.; Roslonek, G.; Taraszewska, J. *J. Electroanal. Chem.* **1996**, *403*, 47.
(12) Pérez-Morales, M.; Muñoz, E.; Martín-Romero, M. T.; Camacho, L. *Langmuir* **2005**, *21*, 5468.
(13) El-Nahass, M. M.; Abd-El-Rahman, K. F.; Darwish, A. A. D. *Mater. Chem. Phys.* **2005**, *92*, 185.
(14) Berríos, C.; Cárdenas-Jirón, G. I.; Marco, J. F.; Gutiérrez, C.; Ureta-Zañartu, M. S. *J. Phys. Chem. A* **2007**, *11*, 2706.
(15) Berríos, C.; Ureta-Zañartu, M. S.; Gutiérrez, C. *Electrochim. Acta* **2007**, *53*, 792.
(16) White, B. A.; Murray, R. W. *J. Electroanal. Chem.* **1985**, *189*, 345.
(17) Li, H.; Guarr, T. F. *J. Electroanal. Chem.* **1991**, *317*, 189.
(18) Santos, A. C.; Zucolotto, V.; Ferreira, M.; Constantino, C. J. L.; Cunha, H. N.; dos Santos, J. R., Jr.; Eiras, C. *J. Solid Electrochem.* **2007**, *11*, 1505.
(19) Gouterman, M. In *The Porphyrins*; Dolphin, D., Ed.; Academic Press: New York, 1978; Vol. III, Part A, Physical Chemistry.
(20) Ortiz, B.; Park, S.-M.; Doddapaneni, N. *J. Electrochem. Soc.* **1996**, *143*, 1800.
(21) Colthup, N. B.; Daley, L. H.; Wiberley, S. E. In *Introduction to Infra Red and Raman Spectroscopy*, 3rd ed.; Academic Press: New York, 1990; Chap 13, p 464.
(22) Scudiero, L.; Barlow Dan, E.; Hipps, K. W. *J. Phys. Chem. B* **2000**, *104*, 11899.
(23) Karweik, D. H.; Winograd, N. *Inorg. Chem.* **1976**, *15*, 2336.
(24) Malinski, T.; Ciszewski, A.; Bennet, J.; Fish, J. R. *J. Electrochem. Soc.* **1991**, *138*, 2008.
(25) Muralidharan, S.; Hayes, R. G. *J. Phys. Chem.* **1979**, *71*, 2970.
(26) Sarno, D. M.; Matienzo, L. J., Jr. *Inorg. Chem.* **2001**, *40*, 6308.
(27) Ghosh, A. *J. Org. Chem.* **1993**, *58*, 6932.
(28) Gassman, P.; Ghosh, A.; Almlöf, J. *J. Am. Chem. Soc.* **1992**, *114*, 990.
(29) Ghosh, A.; Fitzgerald, J.; Gassman, P. G.; Almlöf, J. *Inorg. Chem.* **1994**, *33*, 6057.
(30) Alfredsson, Y.; Brena, B.; Nilson, K.; Ahlund, J.; Kjeldgaard, L.; Nyberg, M.; Luo, Y.; Martensson, N.; Sandell, A.; Puglia, C.; Siegbahn, H. *J. Chem. Phys.* **2005**, *122*, 214723.

JP8046455